Published in final edited form as:
Circulation. 2010 November 16; 122(20): 2031–2038. doi:10.1161/CIRCULATIONAHA.109.866053.

Magnetic Resonance Imaging of Carotid Atherosclerotic Plaque in Clinically Suspected Acute Transient Ischemic Attack and Acute Ischemic Stroke

Jaywant P. Parmar, MD, **Walter J. Rogers, PhD**†, **John P. Mugler III, PhD**, **Erol Baskurt, MD**, **Talissa A. Altes, MD**, **Kiran R. Nandalur, MD**, **George J. Stukenborg, PhD**, **C. Douglas Phillips, MD**, **Klaus D. Hagspiel, MD**, **Alan H. Matsumoto, MD**, **Michael D. Dake, MD**, and **Christopher M. Kramer, MD**

Departments of Radiology (J.P.P., W.J.R., J.P.M., E.B., T.A.A., K.R.N., C.D.P., K.D.H., A.H.M., M.D.D., C.M.K.), Medicine (W.J.R., C.M.K.), Biomedical Engineering (W.J.R., J.P.M.), and Public Health Services (G.J.S.), University of Virginia Health System, Charlottesville; Radiology Associates of San Luis Obispo, San Luis Obispo, Calif (J.P.P.); Department of Radiology, Kaiser Permanente Mid-Atlantic Medical Group, Owings Mills, Md (E.B.); Department of Radiology, William Beaumont Hospital, Royal Oak, Mich (K.R.N.); Department of Radiology, Weill-Cornell Medical College, New York, NY (C.D.P.); and Department of Cardiothoracic Surgery, Stanford University School of Medicine, Stanford, Calif (M.D.D.)

Abstract

Background—Carotid atherosclerotic plaque rupture is thought to cause transient ischemic attack (TIA) and ischemic stroke (IS). Pathological hallmarks of these plaques have been identified through observational studies. Although generally accepted, the relationship between cerebral thromboembolism and in situ atherosclerotic plaque morphology has never been directly observed noninvasively in the acute setting.

Methods and Results—Consecutive acutely symptomatic patients referred for stroke protocol magnetic resonance imaging/angiography underwent additional T1- and T2-weighted carotid bifurcation imaging with the use of a 3-dimensional technique with blood signal suppression. Two blinded reviewers performed plaque gradings according to the American Heart Association classification system. Discharge outcomes and brain magnetic resonance imaging results were obtained. Image quality for plaque characterization was adequate in 86 of 106 patients (81%). Eight TIA/IS patients with noncarotid pathogenesis were excluded, yielding 78 study patients (38 men and 40 women with a mean age of 64.3 years, SD 14.7) with 156 paired watershed vessel/cerebral hemisphere observations. Thirty-seven patients had 40 TIA/IS events. There was a significant association between type VI plaque (demonstrating cap rupture, hemorrhage, and/or thrombosis) and ipsilateral TIA/IS ($P<0.001$). A multiple logistic regression model including standard Framingham risk factors and type VI plaque was constructed. Type VI plaque was the dominant outcome-associated observation achieving significance ($P<0.0001$; odds ratio, 11.66; 95% confidence interval, 5.31 to 25.60).

Correspondence to Jaywant P. Parmar, MD, 380 Main St, Morro Bay, CA 93442. jaywant.parmar@gmail.com.
†Deceased.

Disclosures

Dr Mugler receives research grants and is a consultant for Siemens Healthcare. Dr Kramer receives research equipment support from Siemens Healthcare.

Conclusions—In situ type VI carotid bifurcation region plaque identified by magnetic resonance imaging is associated with ipsilateral acute TIA/IS as an independent identifier of events, thereby supporting the dominant disease pathophysiology.

Keywords

angiography; atherosclerosis; carotid arteries; magnetic resonance imaging; plaque; stenosis; stroke

Because of its ability to image with the use of blood pool contrast techniques, lumenography is now the mainstay in clinical identification and management of coronary, carotid, and peripheral artery atherosclerotic disease. Catheter x-ray arteriography has been the gold standard for stenosis quantification in clinical trials, establishing the benefit of endarterectomy in critical carotid artery stenosis.[1–3] However, lumenographic atherosclerosis imaging has significant limitations. Glagov et al[4] first introduced the concept of positive lumen remodeling, suggesting a preserved lumen despite significant intramural plaque burden. Longitudinal studies of arteriographic coronary artery stenosis subsequently established that lesions <50% more often lead to acute myocardial infarction than stenotic lesions.[5,6] Since these observations were made, the concept has evolved that plaque characteristics may relate better than stenosis to thromboembolic risk. Magnetic resonance imaging (MRI) holds great clinical promise in this regard because of excellent tissue contrast and spatial resolution, as demonstrated by important observational studies incorporating histology.[7–10] Recent advances in 3-dimensional (3D) pulse programming techniques have greatly increased the anatomic accuracy, time efficiency, and overall clinical applicability of high-resolution MRI.[11,12]

A prospective observational study of cerebrovascular events incorporating baseline MRI of the vessel wall among clinically stable patients with carotid stenosis has been reported and is ongoing.[13] MRI-identified risk factors associated with subsequent events include intraplaque hemorrhage and a thin, ruptured fibrous cap.[13,14] To date, no studies have examined carotid plaque characteristics in patients presenting acutely with neurological symptoms compatible with stroke or transient ischemic attack (TIA).

Thus, we hypothesized that MR wall imaging in acutely unstable patients with symptoms of TIA or stroke would help to relate plaque characteristics to the acute clinical event. We utilized efficient MRI pulse sequences and a MRI-modified American Heart Association (AHA) plaque grading method[15] to ascertain the features of fibrous cap disruption, intraplaque hemorrhage, and/or luminal thrombus in situ as they related to ischemic stroke (IS) and TIA occurring within 48 hours of cerebrovascular sign/symptom onset.

Methods

Patient Selection

The research protocol was approved by the local institutional review board. Consecutive hospital and emergency department patients with acute TIA/IS symptoms referred for stroke protocol MRI examination underwent additional research protocol imaging from December 22, 2004, through August 22, 2005. Included clinical referrals were limited to those demonstrating onset of, within 48 hours of MRI stroke protocol examination, a transient or persistent neurological deficit including diminished mental status, aphasia, monocular blindness, and motor and/or sensory deficit. In 25% of cases, the entire examination or the additional sequences were not performed because of absolute (pacemaker) or relative (tremor, claustrophobia) contraindications.

MRI Protocol

High-resolution T1- and T2-weighted black-blood 3D turbo spin echo pulse sequences were developed on site and optimized for use with the clinical stroke protocol receiver coil array. Blood signal suppression ("black blood") was achieved with the use of a standard double-inversion recovery preparation, which combines nonspatially selective and spatially selective radio-frequency pulses. Pulse sequence parameters for the T1-weighted 3D turbo spin echo acquisition included the following: repetition time/echo time, 800/24 ms; echo train length, 27; averages, 2; matrix, 243×448; and pulse sequence parameters for the T2-weighted acquisition included the following: repetition time/echo time, 2000/132 ms; echo train length, 51; number of excitations, 2; matrix, 255×448.[16–18] Both acquisitions used the following: field of view, 12.6×22.0 cm; true in-plane resolution, 0.5×0.5 mm; *z* axis coverage, 66 mm; slice thickness, 3.0 mm reconstructed at 1.5-mm intervals. The additional imaging added 11 minutes 10 seconds to the total examination time.

All studies were single-coil setup routine stroke protocol MRI examinations performed on a Sonata 1.5-T MR scanner (Siemens Medical Solutions, Malvern, Pa) utilizing a commercially available, Food and Drug Administration–approved 3-coil receiver array (birdcage-head, butterfly-neck, and cervical-spine elements). The routine clinical stroke protocol examination excluding the plaque imaging protocol consisted of phase-contrast localizer sequences, axial T1-weighted, axial T2-weighted, axial fluid-attenuated inversion recovery (FLAIR), and axial diffusion-weighted intracranial acquisitions, as well as magnetic resonance angiography (MRA) examinations that included an intracranial 3D time of flight acquisition and an aortic arch through circle of Willis dynamic gadolinium-enhanced, digital mask-subtracted acquisition.

MR Image Review

All clinical hospital services were blinded to the research imaging results. A single reviewer scored image quality from 1 to 5 (5=best) after the stroke protocol examinations. The image clarity was largely dependent on adequate signal-to-noise ratio at vessel depth based on receiver coil positioning, body habitus, and anatomic bifurcation level because these matched with the sensitivity coverage of the inflexible and blindly prepositioned receiver coil arrangement. If 1 bifurcation level was of poor quality, the patient was excluded. To a lesser degree, swallowing motion, respiratory motion, and impulse motion artifacts (only in severely dolichoectatic vessels) limited resolution at the boundaries of coil coverage. Studies with image quality <3 were excluded from further analysis.

Two independent reviewers were blinded to all patient data and complementary imaging. Electronically archived research vessel wall images were reviewed along with corresponding axially reconstructed contrast-enhanced MRA images and a tissue-subtracted contrast-enhanced MRA maximum intensity projection image set. A standardized research display protocol with integrated multiplanar reconstruction tool was utilized.

Atherosclerotic plaque was identified on the basis of the presence of circumferential or eccentric wall thickening. Identified plaques were localized and graded according to the MRI-modified AHA atherosclerotic plaque schema, which condenses the standard of 8 histological types into 6 MR-discernible types. AHA types I and II and types IV and V are combined on the basis of technical limitations of MRI contrast.[15] A maximum intensity projection of the MRA data was used as an overall roadmap and simulated a catheter arteriogram. A consensus scoring between both reviewers was performed after independent scorings on both plaque grading and stenosis degree. Lesions with moderate and critical North American Symptomatic Carotid Endarterectomy Trial stenosis by initial independent

assessment were subject to consensus grading with the use of both visual assessment and geometric analysis.[19]

Specific MRI Grading Method—The tissue grading method was based on prior work in our laboratory[20–25] and details published by others.[8,9,14,15,26–37] The bulk of structural plaque characterization was performed with the use of registered 3D black blood T1 and T2 data sets. General plaque components include lipid-rich core, hemorrhage, acute and organizing thrombus, calcification, and fibrous extracellular connective tissue. The distribution of these components could be defined by multispectral MRI with limitations related to the variable T1 and T2 signal intensity of hemorrhage. Fibrous cap integrity was best identified on axial white blood (contrast-enhanced MRA) images without tissue subtraction.[14] The specific type VI grading was characterized by eccentric or uniform wall thickening with focally increased T1 and/or T2 wall signal intensity displaying a radial inhomogeneity pattern and level of contrast and margin definition that could only be explained by luminal thrombus and/or some element of acute intramural hematoma. Geographically associated penetration of blood into the wall on axially reconstructed MRA data was a very specific finding for type VI characterization. In the case of tandem or long segment plaques, 1 final grade was assigned per side on the basis of the following hierarchy by type: VI, IV/V, VIII, VII, III, and I/II.

Chart Review—After discharge, patient data were abstracted from the fully electronic medical record (CareCast version 2, IDX Systems, Burlingon, Vt) by a chart reviewer blinded to all research imaging data. The emergency medical services/emergency department and/or inpatient chart was evaluated to determine the symptom onset time and cardiovascular risk factors. Brain MRI Digital Imaging and Communications in Medicine time stamps were reviewed to confirm that imaging occurred within 48 hours of symptom onset. Discharge diagnosis was based on hospital discharge summary. In all TIA/IS cases, the Trial of Org 10172 in Acute Stroke Treatment diagnostic classification[38] was used to exclude patient events that were clinically attributable to a cardioembolic event, lacunar stroke, or other non-large-vessel atherosclerotic cause from further analysis. Thus, cryptogenic and large-vessel atherosclerotic lesions were selected as TIA/IS causes for inclusion in hypothesis testing. The complete patient inclusion algorithm is presented in Figure 1. Lateralizing symptoms were identified on the basis of standard clinical diagnostic methods.[39] Aphasia was considered to indicate a left-sided cerebral ischemic event. In cases of IS, diffusion, apparent diffusion coefficient map, T2 FLAIR, and T2-weighted images were assessed to confirm the acuity of the ischemic event.[40,41] In cases of TIA, patients with a clinically documented history of symptoms within 48 hours of imaging were considered positive outcomes. Thereby, cases of acute and hyperacute IS and acute TIA of large-vessel atherosclerotic and undetermined pathogenesis comprised positive outcomes for hypothesis testing.

Data Analysis

SAS version 9 (SAS Institute Inc, Cary, NC) was used for data analysis. Statistical significance was considered to be $P<0.05$. Agreement data were used to quantify reliability, and the final consensus grading data were used to test the pathophysiological hypothesis. Dichotomous κ with a 95% confidence interval (CI) was employed to quantify agreement between the 2 reviewers in the type VI plaque grading. Univariate and multivariate logistic regression models relating TIA/IS prevalence to presence of ipsilateral type VI plaque and Framingham risk factors were created with the use of generalized estimating equation techniques to account for the within-subject correlation.

Results

Of completed studies, 81% (86 of 106 exams) had suitable image quality to be analyzed per protocol. The remaining 20 of 106 studies (19%) were excluded because of poor image quality, primarily due to patient motion.

Of 86 adequate-quality studies, 8 had a known non-large-vessel TIA/IS source: atrial fibrillation with anticoagulation failure (n=3), small-vessel disease (lacunar stroke) (n=2), previously diagnosed hypercoagulable state with anticoagulation failure (n=2), and cerebral arteriovenous malformation (n=1). These patients were excluded as detailed in Figure 1, yielding 78 patients with 156 paired carotid examinations for analysis: 78 right and 78 left plaque-type TIA/IS correlations. A demographic profile including age and cardiovascular risk factors of included patients is presented in Table 1.

The plaque-type frequencies and associated neurological events are detailed in Tables 2 and 3.

Interobserver agreement for type VI grading was found to be 0.52 (95% CI, 0.30 to 0.73) on the left and 0.57 (95% CI, 0.35 to 0.78) on the right. Consensus grading data were used in all secondary analyses.

Thirty-seven patients had events, 3 bilaterally. Twenty-three of 156 carotid examinations demonstrated a type VI plaque with ipsilateral TIA/IS, 11 of 23 with acute TIA (within 48 hours of symptom onset) and 12 of 23 with acute or hyperacute stroke as diagnosed by MRI. Ninety-eight of 156 observations (63%) identified carotid lesions other than type VI in patients who did not have ipsilateral TIA/IS. Eighteen of 156 (11%) were considered false-positive tests demonstrating type VI plaques without TIA/IS outcomes. Seventeen of 156 exams were considered false-negatives without type VI plaque and with TIA/IS. The plaque types observed in these patients consisted of 8 type III, 4 type IV/V, 3 type VII, and, 2 type VIII associated with the neurological sequelae of TIA/IS as described above. The positive predictive value of type VI plaque for TIA/IS was 56%. A negative predictive value of 85% was observed. The association between observation of MRI type VI plaque and ipsilateral outcome of TIA/IS was significant at $P<0.0001$.

In 4 of 156 observations, severe carotid stenosis (70% to 99%) was identified: 3 with ipsilateral TIA/IS (0/3), characterized as type VI, and 1 of 156 without ipsilateral TIA/IS, characterized as type IV/V. Moderate stenosis (30% to 69%) was observed in 9 of 156 sides, of which 3 demonstrated ipsilateral TIA/IS (1/2), all with ipsilateral type VI plaque. The remaining 6 of 9 cases of moderate stenosis did not have TIA/IS, including 3 type VI, 2 type IV/V, and 1 type VII. Mildly stenotic and nonstenotic vessels were observed in the remaining 143 of 156 sides, 16 of which had TIA/IS.

Logistic regressions correcting for within-patient correlation of right- and left-sided arteries with the use of generalized estimating equations were performed, including the presence of ipsilateral type VI plaque and standard cardiovascular risk factors. Ipsilateral type VI plaque was the dominant risk factor ($P<0.0001$; odds ratio, 11.66; 95% CI, 5.31 to 25.60). Current cigarette smoking and age also showed significant associations ($P<0.044$; odds ratio, 2.33; 95% CI, 1.02 to 5.33 for current smoking and $P<0.047$; odds ratio, 1.04; 95% CI, 1.00 to 1.07 for age). No other risk factors reached statistical significance, although all showed a positive correlation. Severe stenosis (70% to 99%) was identified in 4 cases, and this was too infrequent to incorporate into the model with reliability. The detailed results are summarized in Tables 2, 3, and 4.

Discussion

Despite known statistical and pathophysiological limitations,[42,43] lumenographically defined stenosis in combination with a history of TIA/IS remains the standard for identifying clinically significant carotid artery disease. MRI plaque characterization offers improved definition of this heterogeneous disease process, potentially before the onset of symptomatic disease.

In this study of patients imaged for gold standard diagnosis of acute TIA/IS by MRI, we found that MRI-identified type VI atherosclerotic plaque of the carotid bifurcation is strongly associated with ipsilateral acute TIA/IS. By definition, type VI atherosclerotic plaque demonstrates a large burden of extracellular lipid-necrotic material and has associated acute intramural hemorrhage, cap rupture, and/or intraluminal thrombus.[44] Modern pathological models have related this morphology to acute ischemic events. To our knowledge, this is the first large cross-sectional study applying MRI plaque imaging to patients in close temporal association with the onset of symptoms, thereby directly relating the type VI morphology to acute cerebral ischemia of cryptogenic or large-vessel atherosclerotic cause.

These observational data support the concept of plaque vulnerability leading to rupture and thromboembolic ischemic syndromes. Our study population included those clinically identified as having a high probability of acute stroke. As expected, a significant proportion of these patients had an ipsilateral acute diffusion abnormality or received a discharge diagnosis of ipsilateral TIA. A low number of arteries had severe (70% to 99%) luminal stenosis, precluding a statistical analysis. MR plaque characterization demonstrated good accuracy for identification of likely critical lesions. Larger-scale, prospective, and longitudinal studies of MR plaque characterization are needed to determine the accuracy of identification of presymptomatic type IV/V plaques (“vulnerable” state), which may benefit most from aggressive surgical, interventional, medical, or combination therapies.

MR plaque imaging methods have been tested extensively in preclinical models and subsequently studied in patients undergoing carotid endarterectomy, allowing a thorough histological exploration and testing of the techniques. Initial studies included ex vivo research and development to prove techniques on clinical imaging platforms and more recent ex vivo research to extend techniques to intravascular receiver coils.[22] Further testing in vivo in patients scheduled for carotid endarterectomy provided histological correlation. A variety of techniques have been examined in this manner, including contrast-enhanced T1-[21,33] and T2*-weighted[29] imaging. White blood sequences to demonstrate fibrous cap rupture have been found useful in identifying recently symptomatic lesions in an endarterectomy patient series.[14] Overall, studies have demonstrated that multispectral characterization is most accurate.

Prior MR plaque imaging studies have been performed weeks to months after a TIA/IS event, after aggressive medical therapy and significant plaque remodeling. The efficiency of our sequence allowed a complete 3D MR study of the carotid bifurcation in a clinically reasonable time. In this way, we sought to interrogate the ultrastructure of probable culprit plaques in situ predicted by the predominant model of acute disease, which is based on inherently limited surgical pathology. An additional advantage of our method was the increased resolution allowed by the 3D technique. Commonly, small imaging regions of interest most clearly demonstrated the key findings of type VI characterization. Other studies have uniformly utilized 2D imaging techniques that introduce sampling error. The potential advantage of 2D imaging is the ability to define a perpendicular imaging plane relative to the vessel axis orientation, improving resolution of the wall. Certainly, vessel

obliquity frequently resulted in decreased resolution in the present study. However, advances in 3D imaging, use of dedicated surface coils, and parallel acceleration programs will eventually lead to fast isotropic voxel, high-resolution techniques, an important goal.

A recent histological study by Spagnoli et al,[45] focusing on thrombotically active plaque, identified an association between a short interval from symptom onset to carotid endarterectomy and the prevalence of fresh thrombus in the histological specimen. Their data analysis stratified patient cases on the basis of time interval between TIA/IS and carotid endarterectomy. In the 25- to 30-month range, 8 of 18 cases (44%) demonstrated thrombotically active plaque. In the 0- to 2-month group, 32 of 32 cases (100%) demonstrated thrombotically active plaque. Our results confirm this observed association and extend it to the acutely symptomatic time frame (0 to 2 days). Overall, an AHA type VI plaque is equivalent to a thrombotically active plaque, which was observed in a significant proportion of those who suffered large-vessel or undetermined pathogenesis TIA/IS in our study population. However, the question of what lesion preceded the thromboembolic implicated lesion (whether defined as a thrombotically active plaque or type VI lesion) remains.

A limitation of our study is the lack of a gold standard histological reference. Histology will be available rarely in these patients because emergent carotid endarterectomy is not typically performed. In 1 case (Figure 2), we were able to confirm study findings of type VI plaque histologically in a patient with severe stenosis who underwent emergent carotid endarterectomy. This important example serves to demonstrate MRI techniques in acute rupture settings. Another limitation is the lack of a clinical service structured referral for inclusion. All clinical referrals for stroke protocol MRI were considered at our tertiary care center, and neurology service consultation was not required, possibly introducing selection error and bias.

Our plaque-grading technique builds on work of groups that have utilized multiple contrast weightings in plaque characterization. White blood techniques have demonstrated ability in discerning integrity of the fibrous cap both indirectly and directly in conjunction with black blood techniques (Figures 3 and 4). T1- and T2-weighted images with blood signal suppression have always been a mainstay of the techniques. We did not include proton density–weighted imaging. This would have extended patient scanning time and added little information because T2 weighting is most important for characterization purposes.[20,22,31] Other groups utilize single-contrast technique, weighted to be sensitive to T1 or T2* shortening, which is often associated with hemoglobin breakdown.[29,46] We did not employ this technique. Instead, hemorrhage was identified subjectively on the basis of the T1, T2, and white blood images. Our technique may lack the agreement of single-contrast techniques. Nonetheless, we found substantial κ coefficients of agreement between observers for type VI plaque grading: 0.52 on the left and 0.57 on the right. Future isotropic voxel techniques should improve agreement.

Overall, our results demonstrate that MRI methods are clinically effective in the identification of probable culprit carotid bifurcation lesions in patients with suspected acute TIA/IS. Future studies, some currently ongoing,[13] are necessary to determine whether MR plaque characterization can be used to reliably detect presymptomatic lesions at increased risk of rupture.

CLINICAL PERSPECTIVE

Ischemic stroke is a major source of morbidity and mortality in aging populations. The majority of ischemic stroke and precursor events of transient ischemic attack are cryptogenic, and therefore the medical management options for patients who have

suffered transient ischemic attack/ischemic stroke are severely limited. Even after a full acute stroke/transient ischemic attack medical workup, clinicians are often left with no treatable source for the event and are therefore limited to risk factor modification and optimization of medical treatments for diabetes mellitus, hypertension, and hyperlipidemia in patients who are at high risk for subsequent events. Atherosclerosis at the carotid bifurcation is likely the major source for transient ischemic attack/ischemic stroke. The methods to detect critical atherosclerotic disease have essentially been limited to the identification of severely stenotic lesions via lumenography for the last 50 years. Stenotic lesions are uncommon, and a large number of critical lesions are likely being missed because of limitations of atherosclerosis lesion detection and characterization. Through noninvasive magnetic resonance imaging of the vessel wall, both stenotic and nonstenotic American Heart Association type VI atherosclerotic plaque demonstrating intramural hemorrhage, cap rupture, and/or thrombosis in situ can be identified. These type VI lesions are the likely source for cerebral thromboembolism as supported by the leading scientific models of thromboembolic stroke. If critical lesions can be identified, there is an opportunity for medical, surgical, or endovascular treatments of the patients who would benefit most. Furthermore, there would be an opportunity to monitor response to treatment. The potential clinical impact of magnetic resonance imaging of vulnerable carotid bifurcation atherosclerosis is great.

Acknowledgments

The authors acknowledge the critical reviews of Bruce J. Hillman, MD, and the expert technical contributions of Brian Burkholder, RT, and John Christopher, RT.

Sources of Funding

Dr Parmar was supported by a grant from the Radiological Society of North America. Dr Mugler receives research grants and is a consultant for Siemens Healthcare. Dr Kramer receives research equipment support from Siemens Healthcare. He is also supported in part by National Institutes of Health grant 2R01 HL075792.

References

1. Executive Committee for the Asymptomatic Carotid Atherosclerosis Study. Endarterectomy for asymptomatic carotid artery stenosis. JAMA 1995;273:1421–1428. [PubMed: 7723155]
2. North American Symptomatic Carotid Endarterectomy Trial Collaborators. Beneficial effect of carotid endarterectomy in symptomatic patients with high-grade carotid stenosis. N Engl J Med 1991;325:445–453. [PubMed: 1852179]
3. European Carotid Surgery Trialists' Collaborative Group. MRC European Carotid Surgery Trial: interim results for symptomatic patients with severe (70–99%) or with mild (0–29%) carotid stenosis. Lancet 1991;337:1235–1243. [PubMed: 1674060]
4. Glagov S, Weisenberg E, Zarins CK, Stankunavicius R, Kolettis GJ. Compensatory enlargement of human atherosclerotic coronary arteries. N Engl J Med 1987;316:1371–1375. [PubMed: 3574413]
5. Ambrose JA, Tannenbaum MA, Alexopoulos D, Hjemdahl-Monsen CE, Leavy J, Weiss M, Borrico S, Gorlin R, Fuster V. Angiographic progression of coronary artery disease and the development of myocardial infarction. J Am Coll Cardiol 1988;12:56–62. [PubMed: 3379219]
6. Little WC. Angiographic assessment of the culprit coronary artery lesion before acute myocardial infarction. Am J Cardiol 1990;66:44G–47G.
7. Yuan C, Kerwin WS. MRI of atherosclerosis. J Magn Reson Imaging 2004;19:710–719. [PubMed: 15170778]
8. Yuan C, Beach KW, Smith LH Jr, Hatsukami TS. Measurement of atherosclerotic carotid plaque size in vivo using high resolution magnetic resonance imaging. Circulation 1998;98:2666–2671. [PubMed: 9851951]

9. Yuan C, Mitsumori LM, Ferguson MS, Polissar NL, Echelard D, Ortiz G, Small R, Davies JW, Kerwin WS, Hatsukami TS. In vivo accuracy of multispectral magnetic resonance imaging for identifying lipid-rich necrotic cores and intraplaque hemorrhage in advanced human carotid plaques. Circulation 2001;104:2051–2056. [PubMed: 11673345]
10. Saam T, Hatsukami TS, Takaya N, Chu B, Underhill H, Kerwin WS, Cai J, Ferguson MS, Yuan C. The vulnerable, or high-risk, atherosclerotic plaque: noninvasive MR imaging for characterization and assessment. Radiology 2007;244:64–77. [PubMed: 17581895]
11. Mugler JP III, Bao S, Mulkern RV, Guttmann CRG, Robertson RL, Jolesz FA, Brookeman JR. Optimized single-slab three-dimensional spin-echo MR imaging of the brain. Radiology 2000;216:891–899. [PubMed: 10966728]
12. Kallmes DF, Hui FK, Mugler JP III. Suppression of cerebrospinal fluid and blood flow artifacts in FLAIR MR imaging with a single-slab three-dimensional pulse sequence: initial experience. Radiology 2001;221:251–255. [PubMed: 11568348]
13. Takaya N, Yuan C, Chu B, Saam T, Underhill H, Cai J, Tran N, Polissar NL, Isaac C, Ferguson MS, Garden GA, Cramer SC, Maravilla KR, Hashimoto B, Hatsukami TS. Association between carotid plaque characteristics and subsequent ischemic cerebrovascular events: a prospective assessment with MRI: initial results. Stroke 2006;37:818–823. [PubMed: 16469957]
14. Yuan C, Zhang SX, Polissar NL, Echelard D, Ortiz G, Davis JW, Ellington E, Ferguson MS, Hatsukami TS. Identification of fibrous cap rupture with magnetic resonance imaging is highly associated with recent transient ischemic attack or stroke. Circulation 2002;105:181–185. [PubMed: 11790698]
15. Cai JM, Hatsukami TS, Ferguson MS, Small R, Polissar NL, Yuan C. Classification of human carotid atherosclerotic lesions with in vivo multicontrast magnetic resonance imaging. Circulation 2002;106:1368–1373. [PubMed: 12221054]
16. Mugler, JP., III; Kiefer, B.; Brookeman, JR. Three-dimensional T2-weighted imaging of the brain using very long spin-echo trains. Proceedings of the 8th Annual Meeting of ISMRM; Denver. 2000; Berkeley, California: International Society of Magnetic Resonance in Medicine; 2000. p. 687Abstract
17. Merickel MB, Carman CS, Brookeman JR, Mugler JP III, Brown MF, Ayers CR. Identification and 3-D quantification of atherosclerosis using magnetic resonance imaging. Comput Biol Med 1988;18:89–102. [PubMed: 3356147]
18. Mugler, JP., III; Brookeman, JR. Efficient spatially-selective single-slab 3D turbo-spin-echo imaging. Proceedings of the 12th Annual Meeting of ISMRM; Kyoto, Japan. Berkeley, California: International Society of Magnetic Resonance in Medicine; 2004. p. 695Abstract
19. U-King-Im JM, Graves MJ, Cross JJ, Higgins NJ, Wat J, Trivedi RA, Tang T, Howarth SP, Kirkpatrick PJ, Antoun NM, Gillard JH. Internal carotid artery stenosis: accuracy of subjective visual impression for evaluation with digital subtraction angiography and contrast-enhanced MR angiography. Radiology 2007;244:213–222. [PubMed: 17507721]
20. Kramer CM. Magnetic resonance imaging to identify the high-risk plaque. Am J Cardiol 2002;90:15L–17L. [PubMed: 12088772]
21. Kramer CM, Cerilli LA, Hagspiel K, DiMaria JM, Epstein FH, Kern JA. Magnetic resonance imaging identifies the fibrous cap in atherosclerotic abdominal aortic aneurysm. Circulation 2004;109:1016–1021. [PubMed: 14967731]
22. Rogers WJ, Prichard JW, Hu YL, Olson PR, Benckart DH, Kramer CM, Vido DA, Reichek N. Characterization of signal properties in atherosclerotic plaque components by intravascular MRI. Arterioscler Thromb Vasc Biol 2000;20:1824–1830. [PubMed: 10894824]
23. Pearlman JD, Zajicek J, Merickel MB, Carman CS, Ayers CR, Brookeman JR, Brown MF. High-resolution 1H NMR spectral signature from human atheroma. Magn Reson Med 1988;7:262–279. [PubMed: 3205143]
24. Merickel MB, Berr S, Spetz K, Jackson TR, Snell J, Gillies P, Shimshick E, Hainer J, Brookeman JR, Ayers CR. Noninvasive quantitative evaluation of atherosclerosis using MRI and image analysis. Arterioscler Thromb 1993;13:1180–1186. [PubMed: 8343492]
25. Merickel MB, Carman CS, Brookeman JR, Ayers CR. Image analysis and quantification of atherosclerosis using MRI. Comput Med Imaging Graph 1991;15:207–216. [PubMed: 1913571]

26. Aoki S, Nakajima H, Kumagai H, Araki T. Dynamic contrast-enhanced MR angiography and MR imaging of the carotid artery: high-resolution sequences in different acquisition planes. AJNR Am J Neuroradiol 2000;21:381–385. [PubMed: 10696027]
27. Fayad ZA, Fuster V. Characterization of atherosclerotic plaques by magnetic resonance imaging. Ann N Y Acad Sci 2000;902:173–186. [PubMed: 10865837]
28. Hatsukami TS, Ross R, Polissar NL, Yuan C. Visualization of fibrous cap thickness and rupture in human atherosclerotic carotid plaque in vivo with high-resolution magnetic resonance imaging. Circulation 2000;102:959–964. [PubMed: 10961958]
29. Moody AR. Magnetic resonance direct thrombus imaging. J Thromb Haemost 2003;1:1403–1409. [PubMed: 12871274]
30. Shinnar M, Fallon JT, Wehrli S, Levin M, Dalmacy D, Fayad ZA, Badimon JJ, Harrington M, Harrington E, Fuster V. The diagnostic accuracy of ex vivo MRI for human atherosclerotic plaque characterization. Arterioscler Thromb Vasc Biol 1999;19:2756–2761. [PubMed: 10559022]
31. Trivedi RA, U-King-Im J, Graves MJ, Horsley J, Goddard M, Kirkpatrick PJ, Gillard JH. Multi-sequence in vivo MRI can quantify fibrous cap and lipid core components in human carotid atherosclerotic plaques. Eur J Vasc Endovasc Surg 2004;28:207–213. [PubMed: 15234703]
32. Wasserman BA, Haacke EM, Li D. Carotid plaque formation and its evaluation with angiography, ultrasound, and MR angiography. J Magn Reson Imaging 1994;4:515–527. [PubMed: 7949676]
33. Wasserman BA, Smith WI, Trout HH III, Cannon RO III, Balaban RS, Arai AE. Carotid artery atherosclerosis: in vivo morphologic characterization with gadolinium-enhanced double-oblique MR imaging initial results. Radiology 2002;223:566–573. [PubMed: 11997569]
34. Yuan C, Kerwin WS, Ferguson MS, Polissar N, Zhang S, Cai J, Hatsukami TS. Contrast-enhanced high resolution MRI for atherosclerotic carotid artery tissue characterization. J Magn Reson Imaging 2002;15:62–67. [PubMed: 11793458]
35. Coombs BD, Rapp JH, Ursell PC, Reilly LM, Saloner D. Structure of plaque at carotid bifurcation: high-resolution MRI with histological correlation. Stroke 2001;32:2516–2521. [PubMed: 11692010]
36. Mitsumori LM, Hatsukami TS, Ferguson MS, Kerwin WS, Cai J, Yuan C. In vivo accuracy of multisequence MR imaging for identifying unstable fibrous caps in advanced human carotid plaques. J Magn Reson Imaging 2003;17:410–420. [PubMed: 12655579]
37. Zhang S, Cai J, Luo Y, Han C, Polissar NL, Hatsukami TS, Yuan C. Measurement of carotid wall volume and maximum area with contrast-enhanced 3D MR imaging: initial observations. Radiology 2003;228:200–205. [PubMed: 12832583]
38. Adams HP Jr, Bendixen BH, Kappelle LJ, Biller J, Love BB, Gordon DL, Marsh EE III. Classification of subtype of acute ischemic stroke: definitions for use in a multicenter clinical trial: TOAST: Trial of Org 10172 in Acute Stroke Treatment. Stroke 1993;24:35–41. [PubMed: 7678184]
39. Hatano S. Experience from a multicentre stroke register: a preliminary report. Bull World Health Organ 1976;54:541–553. [PubMed: 1088404]
40. Rovira A, Rovira-Gols A, Pedraza S, Grive E, Molina C, Alvarez-Sabin J. Diffusion-weighted MR imaging in the acute phase of transient ischemic attacks. AJNR Am J Neuroradiol 2002;23:77–83. [PubMed: 11827878]
41. Lansberg MG, Thijs VN, O'Brien MW, Ali JO, de Crespigny AJ, Tong DC, Moseley ME, Albers GW. Evolution of apparent diffusion coefficient, diffusion-weighted, and T2-weighted signal intensity of acute stroke. AJNR Am J Neuroradiol 2001;22:637–644. [PubMed: 11290470]
42. Naylor AR, Rothwell PM, Bell PR. Overview of the principal results and secondary analyses from the European and North American randomised trials of endarterectomy for symptomatic carotid stenosis. Eur J Vasc Endovasc Surg 2003;26:115–129. [PubMed: 12917824]
43. Nissen SE, Elion JL, Booth DC, Evans J, DeMaria AN. Value and limitations of computer analysis of digital subtraction angiography in the assessment of coronary flow reserve. Circulation 1986;73:562–571. [PubMed: 3948361]
44. Stary HC, Chandler AB, Dinsmore RE, Fuster V, Glagov S, Insull W Jr, Rosenfeld ME, Schwartz CJ, Wagner WD, Wissler RW. A definition of advanced types of atherosclerotic lesions and a histological classification of atherosclerosis: a report from the Committee on Vascular Lesions of

the Council on Arteriosclerosis, American Heart Association. Circulation 1995;92:1355–1374. [PubMed: 7648691]

45. Spagnoli LG, Mauriello A, Sangiorgi G, Fratoni S, Bonanno E, Schwartz RS, Piepgras DG, Pistolese R, Ippoliti A, Holmes DR Jr. Extracranial thrombotically active carotid plaque as a risk factor for ischemic stroke. JAMA 2004;292:1845–1852. [PubMed: 15494582]
46. Rovira A, Orellana P, Alvarez-Sabin J, Arenillas JF, Aymerich X, Grive E, Molina C, Rovira-Gols A. Hyperacute ischemic stroke: middle cerebral artery susceptibility sign at echo-planar gradient-echo MR imaging. Radiology 2004;232:466–473. [PubMed: 15215546]

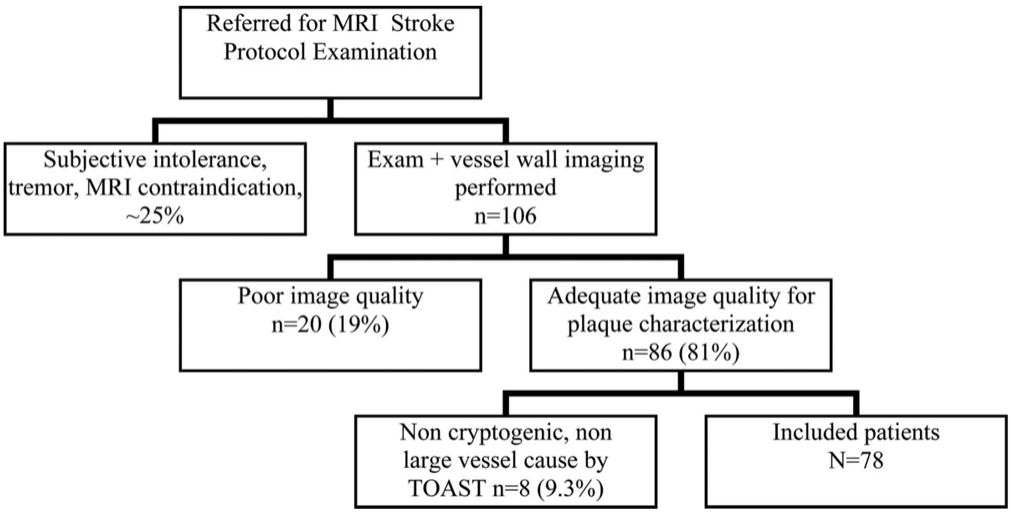

Figure 1.
Eligibility of the subjects included in the analysis. TOAST indicates Trial of Org 10172 in Acute Stroke Treatment.

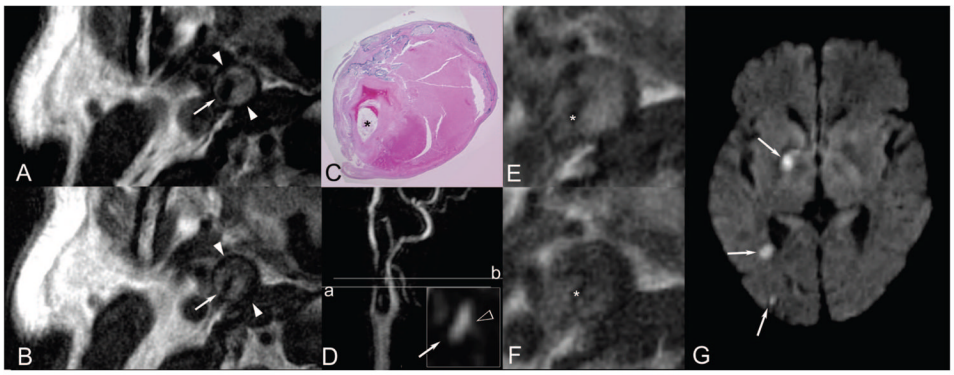

Figure 2.

A through G, Stenotic, ruptured, hemorrhagic/thrombotic type VI atherosclerotic plaque and acute embolic stroke. A 63-year-old man presented with acute onset of left-sided weakness, left neglect, and associated “blackouts.” He was imaged within 48 hours of symptom onset and underwent emergency carotid endarterectomy at 70 hours. A and B, T1- and T2-weighted blood-suppressed MR images demonstrate a large burden of internal carotid artery plaque. Axial sections A and B were obtained at a level indicated by the reference line labeled (a) on D, a maximum intensity projection of the MRA. The inset in image D illustrates axial MRA data at the level (a), with the hollow white arrowhead indicating a focal fading of the contrast column into the vessel wall compatible with the leading edge of a cap rupture. The lumen is indicated by a fine white arrow on A, B, and D (inset). C, E, and F demonstrate a magnification ×10 hematoxylineosin–stained histological section of the endarterectomy specimen in the region of occlusion and corresponding axial T1- and T2-weighted images, all correlating with the reference line labeled (b) on MRA projection (D). These images demonstrate type VI atherosclerotic plaque comprised of hemorrhagic components in various stages of organization, with the lumen indicated (*). Fresh blood is demonstrated in the paraluminal 12 o’clock position, with organizing red and white thrombus demonstrated ranging from the paraluminal 3 (most organized) through 6 o’clock (least organized) positions. Chronic and fibrotic organized thrombus occupies the peripheral wall spanning the 1 through 4 o’clock positions. Calcification is distributed in the extreme peripheral wall circumferentially ranging from the 11 through 3 o’clock positions. The patient suffered multiple acute strokes in the right carotid watershed as demonstrated on the clinical cerebral diffusion-weighted image (G).

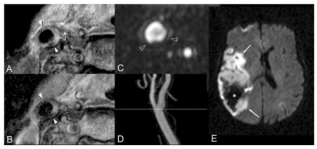

Figure 3.

A through E, Nonstenotic hemorrhagic, thrombotic type VI atherosclerotic plaque, and acute middle cerebral artery territory hemorrhagic stroke. A 77-year-old woman with hypertension, untreated hyperlipidemia, and a current cigarette smoking habit presented with left-sided weakness and mental status changes and was imaged 8 hours from onset. A and B, T1- and T2-weighted axial blood-suppressed MR images demonstrate an abnormal eccentrically thickened right common carotid artery wall as indicated ranging between hollow arrowheads. Radial signal inhomogeneity in this region suggests type VI atherosclerotic plaque. C is axially reformatted 3D MRA data. D is a maximum intensity projection of those data simulating a projectional arteriogram demonstrating no significant luminal stenosis. A reference line indicating the level of A, B, and C is demonstrated. The region of greatest plaque volume as identified on A and B and demarcated between hollow arrowheads on A, B, and C shows heterogeneous intrinsic signal intensity compatible with intramural hemorrhage with a geographically associated focal region of endoluminal irregular contour on C indicating overlying thrombosis in situ and securing the overall classification of type VI. Image E is the clinical cerebral diffusion-weighted image that demonstrates a large acute right hemisphere middle cerebral artery territory hemorrhagic infarction (*).

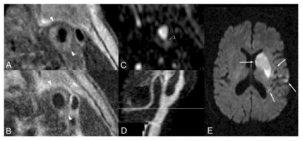

Figure 4.

A through E, Nonstenotic ruptured, hemorrhagic type VI plaque and acute embolic stroke. A 79-year-old man with hypertension presented with acute onset right-sided numbness, weakness, and inability to speak. He was imaged within 28 hours of symptom onset. A and B, T1- and T2-weighted blood-suppressed images demonstrate an abnormally thickened vessel wall with radial signal inhomogeneity suggesting type VI atherosclerotic plaque. C, Axially reformatted 3D MRA data demonstrate contrasted blood extending into the vessel wall as indicated by the arrowhead, tracking circumferentially between the 4 and 8 o'clock positions, a specific sign indicating plaque cap rupture and thereby confirming the type VI classification. The MRA maximum intensity projection (D) demonstrates a focal mild circumferential stenosis at the level of this plaque, indicated by the gray line. A representative section of the clinical cerebral diffusion-weighted image (E) demonstrates multiple acute left middle cerebral artery territory infarctions, indicated by white arrows.

Table 1

Demographic Details for the 78 Evaluated Patients

Variable	No. (or Mean)	Percentage
Type VI atheroma	41 (of 156 carotid observations)	26.3 (of 156 carotid observations)
Male sex	38	48.7
Smoking history	38	48.7
Diabetes mellitus	13	16. 7
Dyslipidemia	36	46.1
Hypertension	58	74.4
Age, y	64.3±14.7	

Table 2

Cervical Carotid Atheroma Incidence, Correlating Dimensional Analysis and Observed Neurological Events of the Study Patients: Correlation of AHA Type VI Plaque Presence With Outcomes of Study Patients

	With TIA/IS	Without TIA/IS	Proportion Affected
With AHA type VI	23	18	0.56
Without AHA type VI	17	98	0.15

Table 3

Cervical Carotid Atheroma Incidence, Correlating Dimensional Analysis and Observed Neurological Events of the Study Patients: Detailed Correlation of Specific AHA Plaque Type With Outcomes of Study Patients

Atheroma Lesion Type	Total No. Observed, Incidence (%)	No. With Neurological Events (TIA/IS)	No. Without Neurological Events	Proportion Affected
AHA type I–II	7 (4)	0	7	0
AHA type III	50 (32)	8 (3/5)	42	0.16
AHA type IV–V	29 (19)	4 (1/3)	25	0.14
AHA type VI	41 (26)	23 (11/12)	18	0.56 (P<0.001)
AHA type VII	12 (8)	3 (2/1)	9	0.25
AHA type VIII	17 (11)	2 (0/2)	15	0.12
70–99% stenosis	4 (2)	3 (0/3)	1	0.75

Table 4

Relative Effects of Various Modeled Risk Factors for TIA/IS in Study Patients

	Unadjusted Odds Ratio	Unadjusted 95% CI Lower Limit	Unadjusted 95% CI Upper Limit	Unadjusted *P*	Adjusted 95% CI Odds Ratio	Adjusted 95% CI Lower Limit	Adjusted 95% CI Upper Limit	Adjusted *P*
Type VI atheroma	12.39	5.14	29.87	<0.0001	11.66	5.31	25.60	<0.0001
Smoking	2.62	1.09	6.30	0.0313	2.33	1.02	5.33	0.0440
Diabetes mellitus	1.13	0.38	3.33	0.8230	0.86	0.20	3.66	0.8355
Dyslipidemia	1.84	0.76	4.41	0.1746	1.94	0.73	5.16	0.1831
Hypertension	3.96	0.92	17.02	0.0645	2.08	0.43	10.13	0.3623
Age in years	1.03	1.00	1.06	0.0211	1.04	1.00	1.07	0.0470